Reducing the ATHENA WFI background with the science products module: lessons from Chandra ACIS

Grant, Catherine, Miller, Eric, Bautz, Marshall, Bulbul, Esra, Kraft, Ralph, et al.

Catherine E. Grant, Eric D. Miller, Marshall W. Bautz, Esra Bulbul, Ralph P. Kraft, Paul Nulsen, David N. Burrows, Steven Allen, "Reducing the ATHENA WFI background with the science products module: lessons from Chandra ACIS," Proc. SPIE 10699, Space Telescopes and Instrumentation 2018: Ultraviolet to Gamma Ray, 106994H (6 July 2018); doi: 10.1117/12.2313864

SPIE.

Event: SPIE Astronomical Telescopes + Instrumentation, 2018, Austin, Texas, United States

Reducing the Athena WFI Background with the Science Products Module: Lessons from Chandra ACIS

Catherine E. Grant[a], Eric D. Miller[a], Marshall W. Bautz[a], Esra Bulbul[b], Ralph P. Kraft[b], Paul Nulsen[b], David N. Burrows[c], and Steven Allen[d]

[a]MIT Kavli Institute for Astrophysics and Space Research, Cambridge, Massachusetts, USA
[b]Harvard-Smithsonian Center for Astrophysics, Cambridge, Massachusetts, USA
[c]The Pennsylvania State University, University Park, Pennsylvania, USA
[d]Department of Physics, Stanford University, Stanford, California, USA

ABSTRACT

The Wide Field Imager (WFI) on ESA's Athena X-ray observatory will include the Science Products Module, a secondary CPU that can perform special processing on the science data stream. Our goal is to identify on-board processing algorithms that can reduce WFI charged particle background and improve knowledge of the background to reduce systematics. Telemetry limitations require discarding most pixels on-board, keeping just candidate X-ray events, but information in the discarded data may be helpful in identifying background events masquerading as X-ray events. We present full frame data from CCDs on-board Chandra, in high-Earth orbit, and the results of our search for phenomenological correlations between particle tracks and background events that would otherwise be categorized as X-rays. In addition to possibly reducing the Athena instrumental background, these results are applicable to understanding the particle component in any X-ray silicon-based detector in space.

Keywords: CCDs, radiation environment, particle background, Chandra, ACIS, Athena, WFI

1. INTRODUCTION

Athena (Advanced Telescope for High ENergy Astrophysics), ESA's next large X-ray observatory, is scheduled to launch in the early 2030s to Earth-Sun L2.[1] Athena will explore the hot and energetic universe using two selectable focal plane instruments. The X-ray Integral Field Unit (X-IFU) will provide spatially resolved high resolution spectroscopy[2] and the Wide Field Imager (WFI) will provide moderate spectroscopy over a large 40 arcminute field of view.[3] The WFI makes use of DEPFET (depleted p-channel field-effect transistor) active pixel sensor arrays with a pixel size of 130 μm $\times$ 130 μm that are fully depleted to 450 μm. The energy range is 0.2–15 keV with a full frame readout time of 5 msec.

As some of the Athena science goals require study of faint diffuse emission, such as that in clusters of galaxies, there has been a substantial effort to better understand, model, and reduce the instrumental background produced by particles and high energy photons, both for the observatory as a whole and for the WFI in particular. The Athena science requirement for the unfocused non-X-ray background is $< 5 \times 10^{-3}$ counts/s/cm^2/keV in the 2–7 keV band and knowledge of the background to within a few percent. The background reduction studies include shielding and coating choices, as well as software mitigation, both on-board and on the ground. A summary of these ongoing efforts by the WFI team is given in Ref. 4.

As part of the U.S. contribution to the WFI, the Science Products Module (SPM) will provide additional on-board processing of the science data stream beyond that being done in the standard WFI event processing.[5] Like most CCD and CCD-like X-ray detectors, full frame pixel data is produced at a rate which is much too rapid to telemeter all the pixels to the ground. The WFI, with 1024 $\times$ 1024 pixels in 4 quadrants and a 5 msec readout time, will output 2×10^8 pixels/second. The WFI standard on-board processing will perform event finding on the full frame images, finding candidate X-ray events and likely discarding pixels that are below a low

Send correspondence to C.E.G., E-mail: cgrant@mit.edu

Space Telescopes and Instrumentation 2018: Ultraviolet to Gamma Ray, edited by Jan-Willem A. den Herder, Shouleh Nikzad, Kazuhiro Nakazawa, Proc. of SPIE Vol. 10699, 106994H · © 2018 SPIE
CCC code: 0277-786X/18/$18 · doi: 10.1117/12.2313864

energy threshold, are above a high energy threshold, or are part of pixel patterns that may be due to particle hits.[6] The remaining candidate X-ray events will then be telemetered to the ground. In this way, much of the non-X-ray background on the detector is eliminated, but some remains as unrejected background events that are masquerading as valid X-ray events. Information in the discarded data may be helpful in identifying the remaining background events. Our goal is to identify on-board processing algorithms that could help further reduce the WFI charged particle background by flagging candidate X-ray events that are most likely associated with the discarded particle tracks.

The U.S. background analysis effort is focused on examining full frame data, both real on-orbit data from a variety of sources and GEANT4 simulated WFI particle background data. In this work, we discuss analysis of Chandra ACIS flight data. A parallel effort is ongoing with the Swift XRT and XMM EPIC-pn.[7] In all cases, we are searching for phenomenological correlations between particle tracks and particle background events that would otherwise be categorized as valid X-rays.

Section 2 describes Chandra ACIS and the full frame data. In Section 3, we outline our methodology for identifying particle tracks and X-ray events, then examine any correlations in our data in Section 4. Finally we discuss our results and plans for future work in Section 5.

2. DATA

For this project we use data from the Advanced CCD Imaging Spectrometer (ACIS)[8] on the Chandra X-ray Observatory,[9] which was launched into a highly elliptical 2.6-day orbit in 1999. We focus on the back-illuminated (BI) CCD, ACIS-S3, as the closest analog of the WFI, but there are substantial structural differences. Most important is the pixel size, 24 μm, and depletion depth, 45 μm, both of which are much smaller than the WFI. Since we are studying the pixel patterns produced by charged particle hits on the detector, the smaller pixels and thinner device will have consequences for our results and how well they translate to the WFI. In addition, the full frame readout time is much longer, seconds versus milliseconds, so the density of particle events in a single frame will be higher.

The data were taken while ACIS was stowed, viewing its External Calibration Source (ECS). No focused X-rays reach the detector—only particles and isolated X-ray lines from the ECS. The ECS produces many spectral features, the strongest of which are Mn-Kα (5.9 keV), Ti-Kα (4.5 keV), and Al-K (1.5 keV), and is powered by the radioactive isotope Fe-55 with a half-life of 2.7 years. The count rate from the ECS, while not negligible, is low enough that the ECS events can be easily identified by energy filtering. Chandra is in a highly elliptical orbit which samples a variety of particle environments, but spends most of its time above the Earth's radiation belts. While the instrument is stowed, the background is dominated by Galactic cosmic rays, primarily protons $>$ 10 MeV, plus any secondary particles produced through interaction with the spacecraft and instrument. Focused low energy protons ($\sim$ 100 keV), which can cause short term increases in background count rates, are not seen while the instrument is stowed. It is expected that the unfocused particle background experienced by Athena should be very similar to that seen in the Chandra stowed data. Further discussion of the sources of the expected WFI background can be found in Ref. 4.

In normal Chandra ACIS operations, only pixels with possible X-ray events are telemetered to reduce data bandwidth. Events that are more likely to be due to particles, such as those with pixels above an upper energy threshold, are discarded onboard. Unlike all standard ACIS observations, the data used in this work were taken in RAW mode, in which there is no on-board bias-correction or event processing and the entire full CCD frame is telemetered to the ground. RAW mode data are taken roughly every six months to help monitor CCD performance and provide a baseline image in case of future instrument anomalies. This is not an efficient mode for collecting event data, as the telemetry bandwidth only allows for $<$ 1% of the full frames to be telemetered, but it is ideal for characterizing the particle background.

We have analyzed 562 ACIS full frames taken during 2003–2016, each with a 3 second exposure. Figure 1 shows two example full frame images, both from November 2016. The mean overclock level was used to remove the bias-pedestal, and then any remaining structure was removed by subtracting the median of each column and row. There is clearly some low-level structure in the example frames, but it is well below any of the thresholds used in finding events or particle tracks. In addition, as this is data from a real instrument there are a small

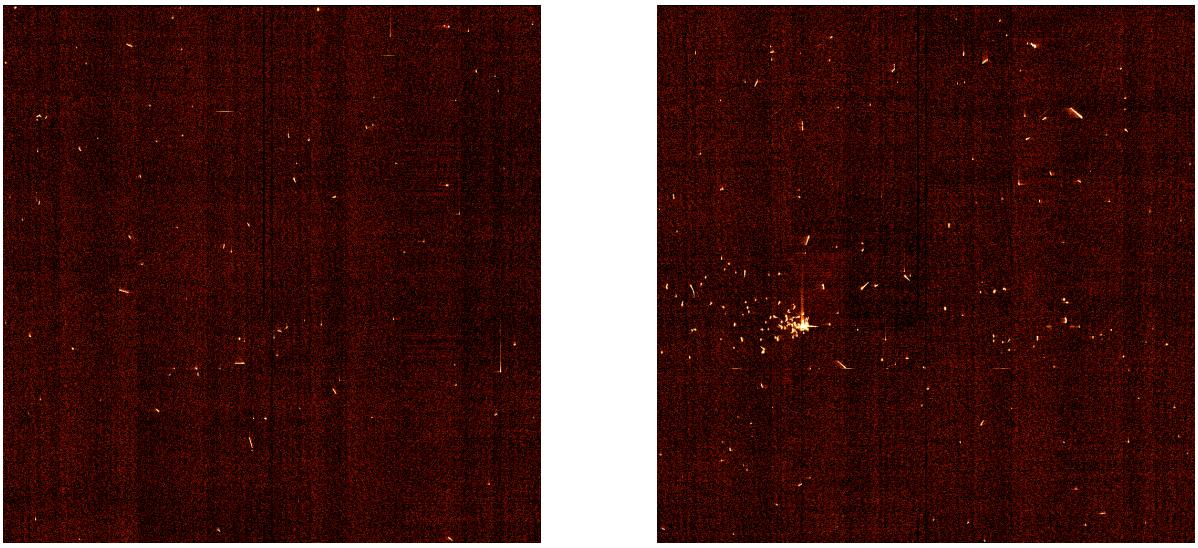

Figure 1: Two example 3 second full frame images from the Chandra ACIS-S3 back-illuminated CCD in November 2016. These data were taken while the instrument was stowed, so there are no cosmic X-rays and the expected count rate from the ACIS calibration source is < 1 count/frame/CCD. All the visible events are due to particles and their secondaries. The right frame shows an extreme example of a cluster of related particle events, presumably due to a single primary particle.

number of hot pixels and columns that must be removed. The brightest pixels also show charge trailing upward due to the detector parallel CTI, and occasional structure in the serial direction due to particle hits during readout. In November 2016, the total count rate from the ECS was < 1 count/frame/CCD, so all of the signal is due to the particle background. The right frame clearly shows a cluster of events, presumably from multiple secondaries associated with a single primary particle. While this is an extreme example, there are other cases where correlations by eye would indicate associations between particle tracks.

3. FINDING PARTICLE TRACKS AND EVENTS

We have analyzed the 562 ACIS full frames to perform event finding and processing, as would be done on-board, and to identify particle tracks. Locations of particle tracks are identified by image segmentation, which finds contiguous sets of > 4 pixels above a threshold value, including connected corners. A single primary particle that produces multiple secondary particles in the instrument would yield multiple particle tracks in the detector. Overlapping tracks would be identified as a single unit. We have identified 31,530 particle tracks in the ACIS full frame data.

Event finding follows the procedure used on-board Chandra ACIS and is similar to most other X-ray CCD instruments. Candidate events are pixels above an event threshold that are also a local maximum of a 3×3 pixel island. The thresholds used for particle track identification and event finding are the same. We find 101,217 total events in our ACIS full frame data. As a particle track can include many pixels over this threshold, there can be multiple events associated with each track. Each event is assigned a grade based on the 3×3 pattern of pixels above a second "split" threshold. We use the ASCA grading scheme, and consider single, and connected double, triple, and quadruple pixel events (G02346) to have acceptable grades that are more likely to be due to X-ray rather than particle interactions. We find 55,685 background events that would be rejected by the grade filter, 12,340 background events that have acceptable, valid event grades, and 33,192 events that are identified by an energy filter as X-ray events from the ACIS calibration source.

In addition, we examine use of the VFAINT mode filter, which has been shown to reduce the background on

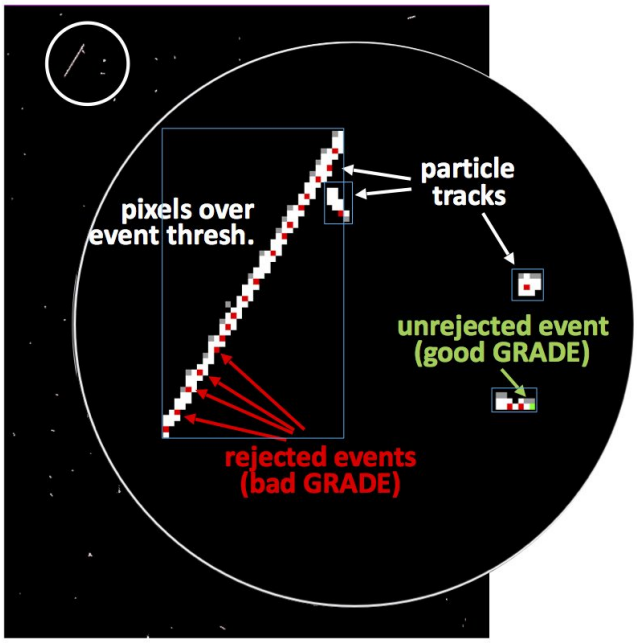

Figure 2: A zoom-in of a region from a full frame ACIS image that contains several particle tracks. White pixels are above the event threshold. Particle tracks found by the image segmentation algorithm are marked by boxes. Events that would be rejected due to their pixel pattern or grade are shown in red. Events that pass a grade filter are categorized as good events and are shown in green.

the ACIS BI CCD by a factor of 1.1–3, depending on energy.* In this mode, a larger 5×5 pixel event island is telemetered for each event. Ground processing can then examine the outer 16 pixels of this 5×5 event island, and further filter out events with signal in those pixels. The efficacy of this filter alone is a strong indication that particle background induced events that would otherwise seem acceptable can be identified by their proximity to nearby signal pixels. There are 7,407 background events in our dataset that have acceptable grades and pass the VFAINT mode filter.

Figure 2 shows an example result of particle track identification and event finding. In this case there are four particle tracks and many events in the zoomed image. Most of the events found associated with the particle tracks would be rejected due to the event grade or pattern and are shown in red. There is, however, an event that would be considered valid based on the grade, shown in green. Additional information about the environments of the event with an acceptable grade would help identify it as due to the particle background.

To validate the results of our particle track identification, we compare their time dependence with another measure of the particle background on ACIS, the rate of events that exceed the high energy threshold. These events are discarded on board, but the number in each frame is telemetered for all ACIS observations. These events have been shown to be well correlated with > 10 MeV protons and are anti-correlated with the solar cycle.[10] Additional small scale dips and transient increases are due to solar storms.

Figure 3 compares the number of particle tracks found in each frame over the 2003–2016 time frame (left) with the rate of high energy rejects over the same time period (right). The high energy rejects have much better coverage, since those data are collected during all ACIS observations. The vertical groupings of particle tracks show many individual data frames taken during two RAW mode observations separated by a few days. There is clear variation on all scales, from seconds between individual data frames, to weeks-long solar events, to the many-year solar cycle.

*http://cxc.harvard.edu/ciao/why/aciscleanvf.html

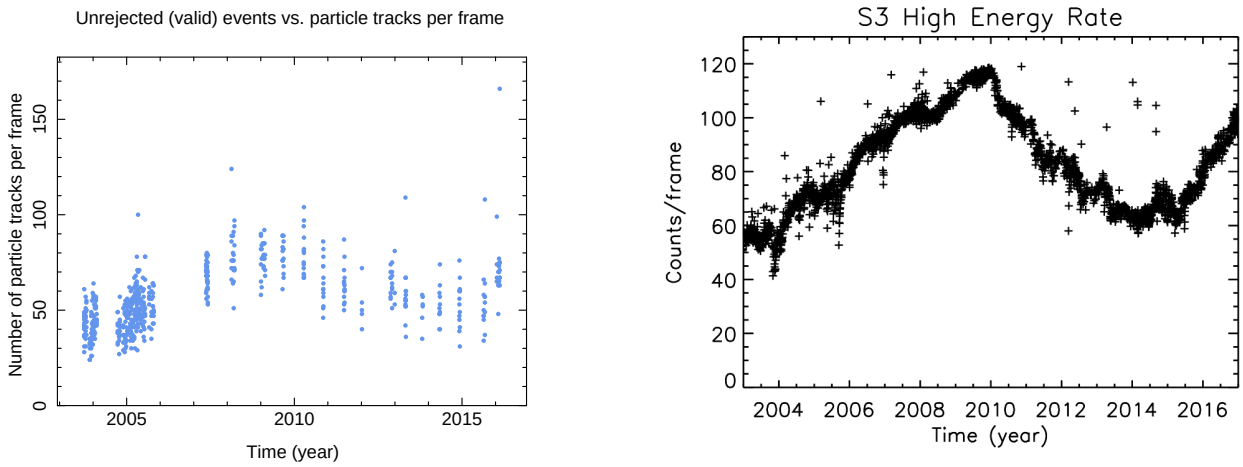

Figure 3: A comparison of the time dependence of particle tracks with another measure of the particle background on ACIS, the rate of rejected high energy events, over the time period 2003–2016. On the left is the number of particle tracks that were identified in each individual 3 second frame. On the right is the average rate of rejected high energy events in every observation of the ACIS calibration source.

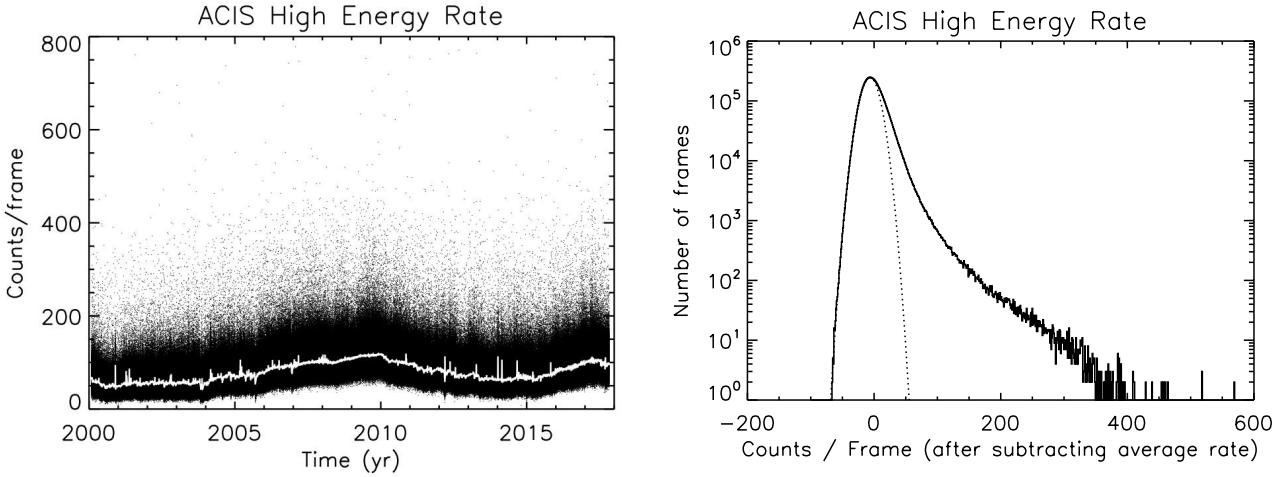

Figure 4: More details on the time dependence of high energy rejected events. On the left is the rate of rejected high energy events in every observation of the ACIS calibration source. The white line shows the average in each observation, while the black dots are the value in each 3 second frame that went into that average. There is substantial variation in the high count rate direction. On the right is a histogram of the count rate in each frame after subtracting the average of that observation to remove the long time scale variation. The high-count-rate tail contains 20% of all frames.

There is a large scatter in the number of particle tracks per frame; some frames have many more particle hits or secondaries than the mean. Figure 4 looks at the high energy reject rate in detail, showing single 3 second frames over the same time period. There is a large variation in the number of high energy events produced by particles in a 3 second frame, with a high-count-rate tail that contains 20% of all frames. This implies there is a higher probability to find particle-induced events in frames with other particle-induced events, of which our putative background reduction algorithm can take advantage.

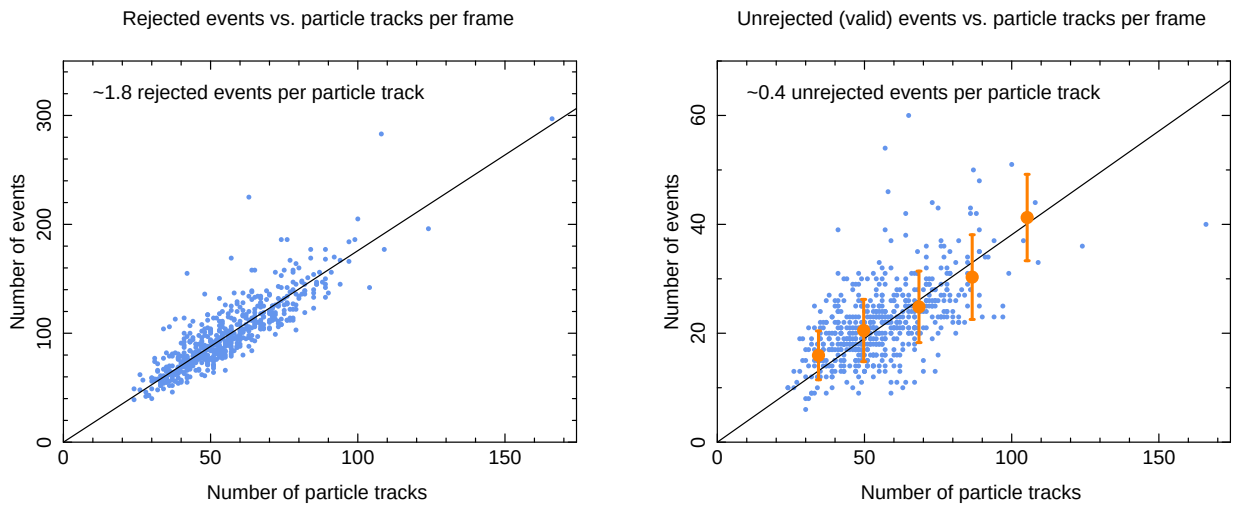

Figure 5: The number of events, both rejected and unrejected, valid events, are well correlated with the number of particle tracks in a frame.

4. CORRELATING EVENTS WITH PARTICLES

Now we compare particle tracks with the events identified by standard processing. Figure 5 shows the number of events with rejected or valid grade patterns as a function of the number of particle tracks in that frame. As expected, the number of rejected events is well correlated with the number of particle tracks, with ~ 1.8 rejected events per particle track. The unrejected events, with grade patterns that would be considered valid X-rays, are also correlated with particle tracks, although the number of events is lower and the correlation is less obvious without binning the data. Particle tracks produce events that look like X-rays at a rate of ~ 0.4 events per particle track.

Next we find the distance between each event and the closest pixel in the nearest particle tracks. Figure 6 is a schematic which shows how our algorithm finds the distance between each event center and particle tracks. We believe the nearest pixels is the cleanest way to define the distance, rather than using a centroid for the particle track or attempting to define a direction for the track.

Both Figures 4 and 5 indicate that unrejected background events should be associated with particle tracks in a single frame. We perform a spatial correlation of particle tracks with the four categories of events: events that were rejected due to their grade, background events with grades that appear to be valid, background events with acceptable grades that also would pass a VFAINT filter, and X-ray events from the ACIS calibration source.

Figure 7 shows the spectra and the spatial correlation with particle tracks for the four categories of events. The spectra for all types of background events have similar energy distributions. The calibration source X-rays in yellow are only found at three distinct energies, by definition. The spatial correlation function on the right shows that all categories of background events are strongly correlated with the particle tracks. This correlation extends well out to 20 or more ACIS pixels from the track. X-rays from the ACIS calibration source show no such correlation, as expected, since they don't know about the spatial position of the particles and are uniformly distributed over the CCD frame. The spatial correlation between valid events and particle tracks argues that filtering the event data by distance to the nearest particle track may be a useful method to reduce the particle background. Preliminary numbers indicate background reduction of up to 75% by removing events within 15 pixels of a particle track.

The WFI is planned to have larger pixels than ACIS (130 μm vs. 24 μm) and a deeper depletion layer (450 μm vs. 45 μm). As both of these will change the pixel patterns produced by charged particle hits on the detector, we also analyzed binned ACIS full frame data, where the native 24 μm pixels are binned by five to 120 μm. This approximates the pixel size of the WFI, but the depletion depth will still be much thinner, so the particle

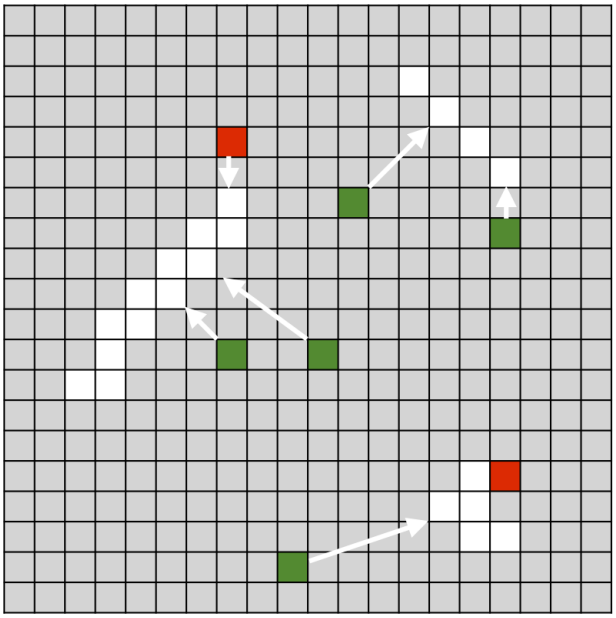

Figure 6: A schematic of how the distance between each event (green and red pixels) and particle track (white pixels) is determined. We find the closest pixel in the nearest particle track and compute the distance to the event center.

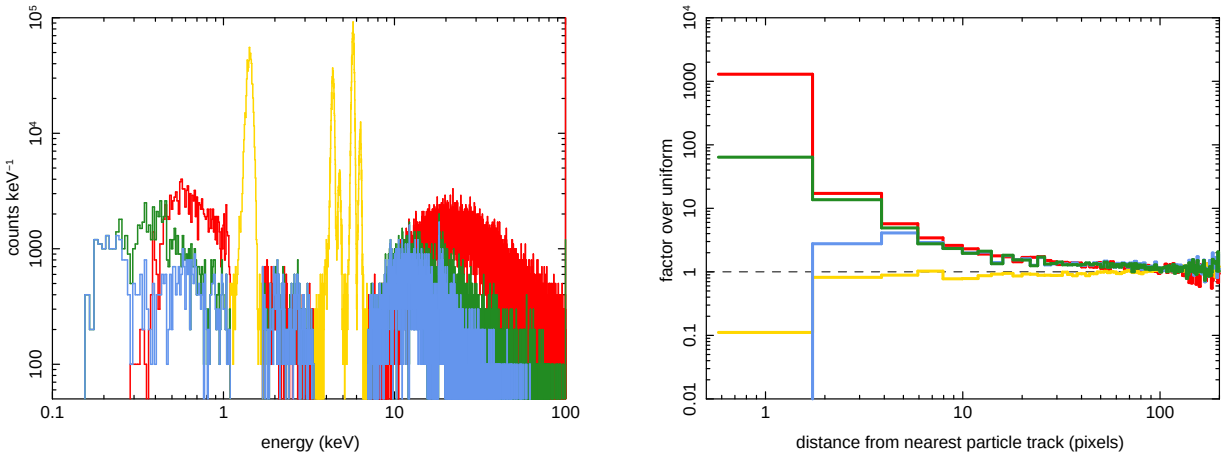

Figure 7: The spectra to the left show the distribution of rejected events (red), unrejected events (green), and unrejected events that pass the VFAINT filter (blue). All types of events have similar energy distributions. X-rays from the ACIS calibration source are also shown in yellow and have been identified by energy. The spatial correlation function for each category of event is shown on the right. All event types, except for the X-rays from the ACIS calibration source, are strongly correlated with the particle tracks.

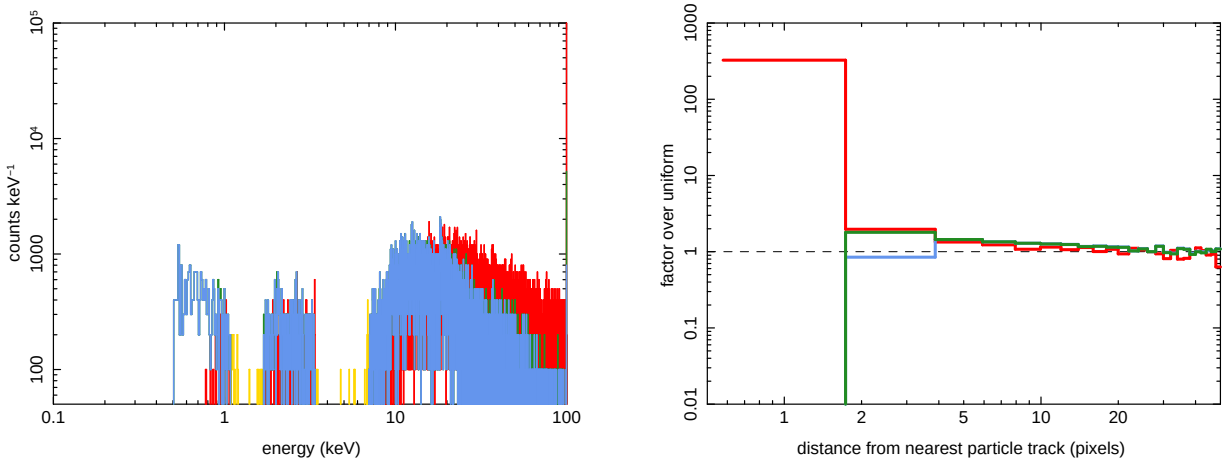

Figure 8: Same as Figure 7, but for ACIS data binned by five to approximate larger 120 μm pixels. The spatial correlation function on the right still shows a correlation of the events with particle tracks.

tracks seen in the binned data will potentially be smaller than those in the real WFI. We performed the same particle track identification, event finding and processing, and spatial correlation on the binned data as discussed previously.

Figure 8 shows the results for the binned data. The threshold used for events and particle tracks is by necessity higher than in the unbinned data, as the effective noise is higher. X-rays from the calibration source have been removed entirely before binning. As binning reduces the distance between particles and events, the spatial correlation is only significant on smaller scales, but is still present out to $\gtrsim 5$ pixels.

We do not have an effective way to simulate the deeper depletion layer on the WFI with our ACIS data. A thicker layer would allow for longer particle tracks, which could be important in the spatial correlation. The thicker depletion layer could also put more energy into individual pixels, which would make them easier to immediately discriminate as particle background events and not X-rays.

5. DISCUSSION AND FUTURE WORK

Substantial work is ongoing by many groups to understand and reduce the charged particle background that will be seen by Athena. We are exploring on-board algorithms that could exploit the full data set from the WFI to better flag particle background events that otherwise would appear to be valid X-rays or to telemeter additional information about the locations of particle tracks. To develop and test these algorithms we have examined on-orbit full frame data from Chandra ACIS taken while the instrument is stowed and not observing the sky. The unfocused particle background seen by ACIS should be similar to what the WFI will experience at Earth-Sun L2. However, structural differences, such as the smaller pixel size and thinner depletion layer, may be important in applying results seen for ACIS to the WFI.

Particles produce candidate events, both events that can be rejected due to their pixel pattern or grade, and events that are masquerading as valid X-ray events. Particle tracks produce events that look like X-rays at a rate of roughly 0.4 event per particle track in the ACIS data. We also find a strong spatial correlation to 20 or more ACIS pixels between these tracks and events, both for the events rejected due to their grade and for the events that would pass grade and VFAINT filters. After spatially binning the data by 5 to better match the WFI pixel size, we find that the spatial correlation persists out to 5+ pixels between particle tracks and events.

In general, we find that on-board particle track identification can reduce the ACIS background and may allow reduction of the WFI background, but further work is required.

A parallel effort by Ref. 7 is examining data from Swift XRT and XMM EPIC-pn. EPIC-pn is a better physical analog to the WFI than ACIS with very similar pixel size and depletion depth, however the data is

from a small window, which restricts the correlation lengths that can be explored. Like the ACIS data, each instrument has its own features and performance characteristics that must be understood and removed from the analysis.

We are also applying the same analysis to GEANT4 simulations of the WFI particle background, as described in Ref. 4. The simulated data by design has precisely the physical characteristics of the real WFI detector, but depends on the accuracy of the physics in the simulation and the mass model of the many structures around the instrument in the spacecraft.

Neither the real data from ACIS and EPIC-pn nor the simulated particle data include astrophysical sources which would be present in the actual WFI data. Any proposed background reduction algorithm must be tested against a more realistic scenario with particle hits and X-ray sources, and any negative impact on the X-ray data must be well understood.

The potential algorithm must be fast enough to run in parallel with the WFI event processor and the expected WFI frame time of 5 millisecond. It must also respond gracefully if count rates are high enough to exceed the resources of the SPM. The result of the on-board analysis would be to add a small amount of additional data for each event to the event list, or at least a flag, which could be used in ground processing to further filter the event list for background reduction.

ACKNOWLEDGMENTS

We gratefully acknowledge support from NASA grant NNX17AB07G, administered by Penn State, and from NASA contracts NAS 8-37716 and NAS 8-38252.

REFERENCES

[1] Nandra, K. et al., "The Hot and Energetic Universe: A White Paper presenting the science theme motivating the Athena+ mission," *ArXiv:1306.2307* (2013).

[2] Barret, D. et al., "The Athena X-ray Integral Field Unit (X-IFU)," in [*Space Telescopes and Instrumentation 2016: Ultraviolet to Gamma Ray*], *Proc. SPIE* **9905**, 99052F (2016).

[3] Meidinger, N. et al., "The Wide Field Imager instrument for Athena," in [*UV, X-ray, and Gamma-Ray Space Instrumentation for Astronomy XX*], *Proc. SPIE* **10397**, 103970V (2017).

[4] von Kienlin, A. et al., "Evaluation of the ATHENA/WFI instrumental background," in [*Space Telescopes and Instrumentation 2018: Ultraviolet to Gamma Ray*], *Proc. SPIE* **10699**, 1069953 (2018).

[5] Burrows, D. et al., "The ATHENA WFI science products module," in [*Space Telescopes and Instrumentation 2018: Ultraviolet to Gamma Ray*], *Proc. SPIE* **10699**, 1069954 (2018).

[6] Plattner, M. et al., "WFI electronics and on-board data processing," in [*Space Telescopes and Instrumentation 2016: Ultraviolet to Gamma Ray*], *Proc. SPIE* **9905**, 99052D (2016).

[7] Bulbul, E. et al., "Characterizing particle background of ATHENA WFI for the Science Products Module: Swift XRT Full Frame and XMM-PN Small Window Mode Observations," in [*Space Telescopes and Instrumentation 2018: Ultraviolet to Gamma Ray*], *Proc. SPIE* **10699**, 10699157 (2018).

[8] Garmire, G. P., Bautz, M. W., Ford, P. G., Nousek, J. A., and Ricker Jr., G. R., "Advanced CCD Imaging Spectrometer (ACIS) instrument on the Chandra X-ray Observatory," in [*X-Ray and Gamma-Ray Telescopes and Instruments for Astronomy*], Truemper, J. E. and Tananbaum, H. D., eds., *Proc. SPIE* **4851**, 28–44 (2003).

[9] Weisskopf, M. C. et al., "An Overview of the Performance and Scientific Results from the Chandra X-Ray Observatory," *Pub. of the Astron. Society of the Pacific* **114**, 1–24 (2002).

[10] Grant, C. E., Bautz, M. W., and Virani, S. N., "The temporal characteristics of the Chandra X-ray Observatory high energy particle background," in [*The High Energy Universe at Sharp Focus: Chandra Science*], Schlegel, E. M. and Vrtilek, S. D., eds., *ASP Conf. Ser.* **262**, 401–407 (2002).